

Non-Energetic Reactive Armor (NERA) and Semi-Energetic Reactive Armor (SERA) FY 13 Final Report

Andrew Robinson
Nikki Rasmussen
Ben Langhorst

August 2013



The INL is a U.S. Department of Energy National Laboratory
operated by Battelle Energy Alliance

DISCLAIMER

This information was prepared as an account of work sponsored by an agency of the U.S. Government. Neither the U.S. Government nor any agency thereof, nor any of their employees, makes any warranty, expressed or implied, or assumes any legal liability or responsibility for the accuracy, completeness, or usefulness, of any information, apparatus, product, or process disclosed, or represents that its use would not infringe privately owned rights. References herein to any specific commercial product, process, or service by trade name, trade mark, manufacturer, or otherwise, does not necessarily constitute or imply its endorsement, recommendation, or favoring by the U.S. Government or any agency thereof. The views and opinions of authors expressed herein do not necessarily state or reflect those of the U.S. Government or any agency thereof.

**Non-Energetic Reactive Armor (NERA) and
Semi-Energetic
Reactive Armor (SERA)
FY 13 Final Report**

**Andrew Robinson
Nikki Rasmussen
Ben Langhorst**

August 2013

**Idaho National Laboratory
National and Homeland Security
Idaho Falls, Idaho 83415**

<http://www.inl.gov>

**Prepared for the
U.S. Department of Energy
Through the INL LDRD Program
Under DOE Idaho Operations Office
Contract DE-AC07-05ID14517**

CONTENTS

1.	INTRODUCTION	1
2.	METHODS.....	1
2.1	Target Groups	1
2.2	Ballistic Testing	3
3.	RESULTS.....	5
3.1	Shot List.....	5
3.2	Target Performance – Residual Mass data.....	6
3.3	Target Plate Erosion.....	6
3.4	Burn Velocities	7
3.5	High Speed Video Analysis	7
4.	DISCUSSION.....	11
4.1	Residual Mass	11
4.2	Deflagration Velocity.....	11
4.3	High Speed Video	11
4.4	Real Time Video	12
5.	CONCLUSIONS	12
6.	REFERENCES	12
	APPENDIX A.....	13

FIGURES

Figure 1.	Cross-section of an uncompressed rubber target.....	2
Figure 2.	Cross-section of a compressed rubber target.....	2
Figure 3.	Array of energetic tiles that was sandwiched between two 0.25-in. thick RHA plates to form the SERA targets.....	3
Figure 4.	Target setup featuring 60-degrees of obliquity and a soft-catch box behind the target.....	4
Figure 5.	Sabot and rod used for ballistic testing.....	4
Figure 6.	Residual mass data is plotted as a function of line-of-shot areal density. Prior test data from monolithic RHA targets tested with no obliquity is also shown. Generally, residual mass decreases with line-of-shot areal density, which is to be expected. No other outstanding trends were observed.	6
Figure 7.	High-speed photo frames from an uncompressed rubber target (shot 2).....	8
Figure 8.	High-speed photo frames from a semi-energetic (50/50) target (shot 11).....	9
Figure 9.	High-speed photo frames from a semi-energetic (70/30) target (shot 8).....	10

Figure 10. Front and back plates from a shot 70/30 SERA target with lines depicting where break lines were positioned. 14

Figure 11. Front and back plates from a shot 70/30 SERA target with lines depicting where break lines were positioned 15

Figure 12. Front and back plates from a shot 50/50 SERA target with lines depicting where break lines were positioned. 16

TABLES

Table 1. Pressed energetic tile statistics. 3

Table 2. List of Ballistic Test Events with Relevant Target Performance Data. 5

Table 3. Post-test measurements of target front- and rear-plate masses. 7

Table 4. Energetic Layer Burn Velocities. 7

ACRONYMS

Non-Energetic Reactive Armor (NERA) and Semi-Energetic Reactive Armor (SERA) FY 13 Final Report

1. INTRODUCTION

INL researchers have proposed prototypes for future lightweight armor systems that reside in a technology gap between explosive-reactive armor and passive armor. The targets were designed to react under impact and throw a steel front plate into the path of the projectile, forcing the projectile to engage more of the front plate during its penetration process. These prototypes are intended to exhibit the enhanced efficiency of explosive reactive armor without the collateral damage often associated with explosive reactive armor.

One of the prototype systems, Semi-Energetic Reactive Armor (SERA), functions similarly to explosive reactive armor, but features a reactive material that reacts much slower than explosive reactive armor. Two different SERA test groups were built and featuring different ratios of aluminum-Teflon[®] powders pressed into 0.5-in.-thick energetic tiles and sandwiched between 0.25-in.-thick RHA plates.

The other prototype system, Non-Energetic Reactive Armor (NERA), utilizes the strain energy in compressed rubber to launch a front flyer plate into the path of an incoming projectile. It is comprised of a 1-in.-thick rubber layer sandwiched between two 0.25-in.-thick RHA plates with bolt holes around the perimeter. Bolts are inserted through the entire target and tightened to compress the rubber sheet to significant strain levels (~40%). A fourth group of targets was tested as a control group. It featured a 0.5-in.-thick rubber sheet sandwiched between two 0.25-in.-thick RHA plates, similar to the NERA test articles, but the rubber is uncompressed.

The four test groups (uncompressed rubber, compressed rubber, 70/30 Al/PTFE, 50/50 Al/PTFE) were each fabricated with three identical test articles in each group. All twelve targets were subjected to ballistic testing at the National Security Test Range on July 17, 2013. They were tested with 0.5-in. diameter steel rods shot at a consistent velocity at each target. In order to characterize the energetic materials, break wires were embedded in the targets and burn velocities were measured. The residual mass method was used to compare the target performance of each group and final performance data is presented below.

2. METHODS

2.1 Target Groups

Four target variants were constructed and tested. Their front surfaces each measured 6 × 12 in., but they were tested with 60-degrees of obliquity, so they presented 6 × 6 in. of line-of-site frontal surface area. The four groups were:

Uncompressed Rubber (control group)

- 0.25-in.-thick RHA Plate
- 0.5-in.-thick Natural Gum Rubber
- 0.25-in.-thick RHA Plate.



Figure 1. Cross-section of an uncompressed rubber target.

Compressed Rubber Target

- 0.25-in.-thick RHA Plate
- 1.0-in.-thick Natural Gum Rubber
- Compressed to 0.6in. thick using sixteen 1/4-20
- Bolts around the perimeter of the target
- 0.25-in.-thick RHA Plate.



Figure 2. Cross-section of a compressed rubber target.

Low Burn Velocity Semi-Energetic Target

- 0.25-in.-thick RHA Plate
- 0.5-in.-thick layer of energetic tiles
- 70/30 weight ratio of aluminum and Teflon©
- 0.25-in.-thick RHA Plate.

High Burn Velocity Semi-Energetic Target

- 0.25-in.-thick RHA Plate
- 0.5-in.-thick layer of energetic tiles
- 50/50 weight ratio of aluminum and Teflon©
- 0.25-in.-thick RHA Plate.



Figure 3. Array of energetic tiles that was sandwiched between two 0.25-in. thick RHA plates to form the SERA targets.

RHA plates were procured from Clifton Steel to Mil Spec 12560.

Natural Gum Rubber sheets were procured from McMaster-Carr. The rubber sheets that were compressed were cut to be smaller than the RHA plates, so they would have room to squish and bulge under compression without interfering with the bolts around the perimeter.

Energetic tiles were custom-fabricated at INL for this specific project. The energetic material used was an aluminum-Teflon[®] mixture, which has been used by others as a very insensitive energetic material. Aluminum powder was procured from Valimet (H-5 powder, 8 μm) and Teflon[®] powders were procured from 3M (Dyneon PTFE, TF-1750, 20 μm). The Teflon[®] was screened to breakup any large clumps. Then the two powders were slurried together in acetone, and dried overnight. The dried powder was pressed into 68.5-g tiles measuring 1.997-in. by 1.997-in. and roughly 0.5-in. thick. Pressing was conducted on July 16, 2013 at INL's National Security Test Range using a 100-ton press and a set of 2-in. square pressing dies from Across International. 44,000-lb (+/-8,000-lb) of force were applied to loose powder to make each tile. 18 tiles were pressed for each target. Table 1 presents the relative densities, absolute densities, and weights of the groups of tiles fabricated.

Table 1. Pressed energetic tile statistics.

Al/PTFE Composition (count)	Relative Density (%)		Density (g/cc)		Weight (g)	
	Average	St. Dev.	Average	St. Dev.	Average	St. Dev.
70/30 (54)	82.6%	1.0%	2.11	0.03	68.48	0.29
50/50 (54)	86.8%	0.9%	2.13	0.02	68.65	0.47

2.2 Ballistic Testing

All ballistic testing was conducted on July 17, 2013 at the National Security Test Range.

Targets were placed on a reusable test frame that held the targets at a steep angle to provide 60-degrees of obliquity. Behind the target, sheet rock and dry rags were packed tightly in a plywood box to soft-catch the residual projectile after it perforated the target. To improve the density of the packed rags, heavy steel plates were placed on top of the rags.



Figure 4. Target setup featuring 60-degrees of obliquity and a soft-catch box behind the target.

INL's residual mass method was used to compare performance of the alternative target groups. The residual mass method is an efficient means of developing comparative performance metrics with relatively few experimental tests. It involves fully perforating targets with a consistent projectile traveling at a consistent velocity and recovering the residual projectile in a soft-catch behind the target. The mass of the residual projectile is measured and the performances of different armor groups are compared using the residual masses, with lower residual masses correlating with better armor performance.

Three of the semi-energetic targets were instrumented with break-wires to help measure the burn velocity of the energetic material. The break wires were each wired into a circuit with a 10k-ohm resistor and a 9-volt battery. The voltage across the circuit was measured by the meDAQ system at a sample rate of 2M samples per second. Break wires were positioned in 2-in. increments so that researchers could observe how the burn velocity changed as the reaction propagated through the target.

Two high-speed cameras were setup to capture (a) a close-up view of the impact event and (b) a wider view of the test pad during the event. A real-speed camcorder was positioned a safe distance away from the event to record the sights and sounds of the events. This enabled qualitative comparisons between non-energetic and semi-energetic variants – specifically comparisons of reaction violence and collateral damage. Oehler M57 light screens were connected to an Oehler M83 ballistic chronograph to measure incoming projectile velocity.

Projectiles were launched from INL's 30-mm test canon. The projectile was an S7 tool steel rod measuring 0.5-in. in diameter, and 5-in. long (10:1 aspect ratio). The rod weighed 1946 grains and the total sabot and projectile package weighed 3563 grains. The sabot was Ben's "10-1 Steel Rod Sabot Design." The rod and sabot were propelled by 2,500 grains of IMR-4895 smokeless powder.



Figure 5. Sabot and rod used for ballistic testing.

3. RESULTS

Thirteen shots were conducted. The first shot was a warm-up shot featuring a dummy sample. The following 12 shots were tests of the four different test groups. A variety of measurements were made during and after testing and are presented below. As a metric of target performance, the residual rod mass was measured and normalized by incoming kinetic energy. In order to examine potential differences in the degree to which the front plates were being forced to engage with the projectile, the residual masses of the plates were measured and are presented below. For three of the SERA targets, energetic material burn velocities were calculated using the break-wire data captured by the meDAQ.

The reaction violence was qualitatively observed by examining the target frame after each test. Each baseline target, NERA target, and SERA target was observed to slightly dent or deform the target frame, but none of the targets caused significant damage to the test frame that required any repairs. All twelve tests were conducted without repairing the test frame. For comparison, a single explosive-reactive armor that would be expected to cause significant and permanent damage to the test frame, including denting, bending, and possibly fracturing the arms of the test frame that directly contacted the targets.

3.1 Shot List

Table 2. List of Ballistic Test Events with Relevant Target Performance Data.

Shot No.	Velocity (ft/sec)	Projectile Pitch (degrees)	Target Name	Line-of-Shot Areal Density (lb/sq.ft)	Impact Kinetic Energy (kJ)	Residual Rod Mass (grains)	Residual Rod Mass / Kinetic Energy
2	3605	2.2	Uncompressed Rubber A	45.62	76.1	904	71.49
3	3634	3.3	Uncompressed Rubber B	45.62	77.4	--	--
4	3595	4.5	Uncompressed Rubber C	45.62	75.7	744*	59.16*
5	3579	4.0	Compressed Rubber A	50.41	75.0	806	64.67
6	3631	1.5	Compressed Rubber B	50.41	77.2	834	65.01
7	3587	3.8	Compressed Rubber C	50.41	75.4	868	69.33
8	3592	2.1	70/30 Al/PTFE A	51.63	75.6	802	63.88
9	3666	0.3	70/30 Al/PTFE B	51.63	78.7	892	68.21
10	3605	3.9	70/30 Al/PTFE C	51.63	76.1	764	60.42
11	3613	3.3	50/50 Al/PTFE A	51.63	76.5	1306**	102.82**
12	3623	2.6	50/50 Al/PTFE B	51.63	76.9	762	59.66
13	3642	3.2	50/50 Al/PTFE C	51.63	77.7	848	65.71

* This data point is excluded from further analysis. The residual rod impacted a steel plate at the top of the soft-catch box. This "secondary" impact occurred at a low velocity, but likely caused additional erosion or fracture of the residual projectile.

** This data point is excluded from further analysis. The residual rod wrapped itself around a small piece of target material and the two pieces could not be disconnected. Thus the residual mass is exaggerated and inaccurate.

3.2 Target Performance – Residual Mass data

Residual Mass was measured for each test. Two of the residual masses were deemed outliers: during Shot 4, the residual rod impacted a steel plate at the top of the soft-catch box. This “secondary” impact occurred at a low velocity, but likely caused additional erosion or fracture of the residual projectile. During Shot 11, the residual rod wrapped itself around a small piece of target material and the two pieces could not be disconnected. Excluding those two data points, the remaining data were plotted in Figure 6 as a function of line-of-shot areal density.

The lowest areal density targets tested were the uncompressed rubber targets. The compressed rubber targets featured an extra 0.5-in. of rubber squished into the sandwich so the areal density is slightly higher. The density of the energetic materials were slightly higher than the density of rubber so targets featuring the energetic tiles in the center had slightly higher line-of-shot areal densities. The densities of the two different energetic compositions were nearly identical, so their targets also featured nearly identical line-of-shot areal densities.

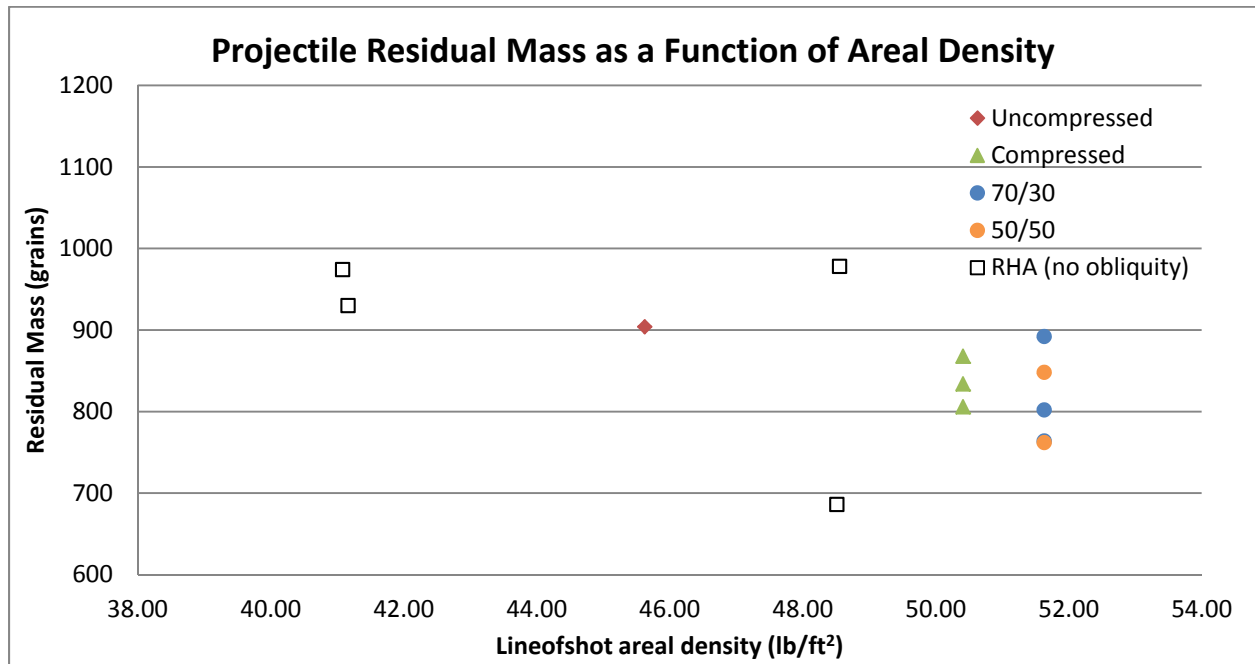


Figure 6. Residual mass data is plotted as a function of line-of-shot areal density. Prior test data from monolithic RHA targets tested with no obliquity is also shown. Generally, residual mass decreases with line-of-shot areal density, which is to be expected. No other outstanding trends were observed.

3.3 Target Plate Erosion

Each front and rear plate was weighed after testing to examine potential differences in the degrees to which plates were forced to interact with the projectile during the penetration process. The bolts of the compressed rubber targets need to be cut to separate the front and rear plates, so they have not yet been measured. The plates were qualitatively examined for patterns between test groups and no patterns were observed in terms of petaling, bulging, or overall deformation.

Table 3. Post-test measurements of target front- and rear-plate masses.

Target Name	Front Plate Post-Test Weight (grains)	Rear Plate Post-Test Weight (grains)	Total Front + Rear Plate Post-Test Weight (grains)
Uncompressed Rubber A	36668	37200	73868
Uncompressed Rubber B	35906	36802	72708
Uncompressed Rubber C	36528	37398	73926
70/30 Al/PTFE A	36966	36748	73714
70/30 Al/PTFE B	36180	37224	73404
70/30 Al/PTFE C	36700	37562	74262
50/50 Al/PTFE A	37450	36322	73772
50/50 Al/PTFE B	37814	37482	75296
50/50 Al/PTFE C	36744	36534	73278

3.4 Burn Velocities

Break-wire measurements are presented in the Appendix for each of the three shots that were instrumented. Using the break-wire data, arrival times were estimated at each wire and the arrival times are plotted with break-wire position data to allow researchers to estimate reaction velocities. Precise determination of break-times was a critical task. Attempts were made to automate the process by setting thresholds for absolute voltage changes or slope changes, but the most accurate method proved to be visual assessment. Burn Velocities were generally observed to decay as the reaction progressed. This is likely due to decreasing confinement and the dissipation of the ballistic impact. Using the multiple arrival time data points, polynomial best-fit curves were fit to the data and initial velocities in the impact zone were calculated from the best-fit equations.

Table 4. Energetic Layer Burn Velocities.

Shot Number	Al/PTFE Composition	Initial Burn Velocity (ft/sec)
9	70/30	1699. 80
10	70/30	2475. 69
12	50/50	2412. 38

3.5 High Speed Video Analysis

The following figures present images from high-speed video of the impacts accompanied by explanations of the events as they are occurring.

High Speed Video Frame	Time After Impact	
	-68 μ s	Rod is just about to impact target.
	+15 μ s	Flash seen is due to the collision of the projectile tip with the target face under very high strain rates.
	+98 μ s	Projectile and target debris is exiting the penetration hole.
	+181 μ s	As the sabot and pusher plate strike the target, more debris is generated. Some of the plastic sabot parts may actually be combusting in this frame as they slide up the target like a ramp.
	+264 μ s	
	+347 μ s	
	+430 μ s	The cloud of spall products decays further as it exits the frame to the upper left. Note the thin line in the rubber layer from shock wave motion.
	+513 μ s	The cloud of spall products leaves the frame, and the residual shock wave within the rubber continues to bounce between the steel plates.

Figure 7. High-speed photo frames from an uncompressed rubber target (shot 2).

High Speed Video Frame	Time After Impact	
	-61 μ s	Rod and sabot are just about to impact target.
	+22 μ s	Flash seen is due to the collision of the projectile tip with the target face under very high strain rates.
	+105 μ s	The rod is roughly halfway through the target. It may be possible that the Al-PTFE reaction has begun here due to the brightness difference/size of flash at +105 μ s when compared to Figure 7 at +98 μ s.
	+188 μ s	Al-PTFE reaction products are beginning to emerge from the impact location, and two separate flashes can be seen segregating themselves (one from penetration events, and one from the Al-PTFE reaction).
	+271 μ s	Further evolution of the Al-PTFE reaction is seen. Note the further segregation of the flashes, and the higher brightness at +271 μ s when compared to Figure 9.
	+354 μ s	
	+437 μ s	Further evolution of the Al-PTFE reaction is seen. Note the apparent lack of movement in the front plate even at this relatively late stage in the reaction process.
	+520 μ s	Further evolution of the Al-PTFE reaction is seen. Note the absence of a front plate visual. If thrown, it would be visible high, and in the center of the frame, but it is still within the cloud and obscured.

Figure 8. High-speed photo frames from a semi-energetic (50/50) target (shot 11).

High Speed Video Frame	Time After Impact	
	-61 μ s	Rod and sabot are just about to impact target.
	+22 μ s	Flash seen is due to the collision of the projectile tip with the target face under very high strain rates.
	+105 μ s	The projectile is approximately half way through, and the “dull” flash shown is from the projectile/sabot melting/combusting.
	+188 μ s	The spall from the projectile impact is thrown up the target like a ramp towards the upper left of the image as the rod finishes penetrating the target completely. So far, the impact sequence is analogous to Figure 7 (base armor) at +181 μ s.
	+271 μ s	This is the first visual evidence of the Al-PTFE reacting. In the middle of the target, the reaction is seen as a separate ball of flame coming from the hole formed by the projectile.
	+354 μ s	The majority of the flash in the frame is now a product of the Al-PTFE reaction which is evolving from the impact location.
	+437 μ s	Evolution of the Al-PTFE reaction is seen. Note the apparent lack of movement in the front plate despite the obvious reaction of the Al-PTFE progressing.
	+520 μ s	Further evolution of the Al-PTFE reaction is seen. Again, note the lack of movement in the front plate despite the progression of the Al-PTFE reaction.

Figure 9. High-speed photo frames from a semi-energetic (70/30) target (shot 8).

4. DISCUSSION

4.1 Residual Mass

The residual rod mass method was used as the primary method to quantify the prototype armor effectiveness. Residual mass results show that the NERA and SERA prototype armor concepts exhibited similar projectile erosion efficiency. The SERA targets outperformed the NERA targets and they both outperformed the baseline targets, but the better performing targets were also slightly heavier. These tests were conducted at 60-degrees of obliquity, and INL researchers currently don't have any other 60-degree obliquity test data available for comparison. However, monolithic RHA targets have been tested with the same projectiles at the same velocities with no obliquity, so this data is plotted in Figure 6 to provide a frame of reference in the tradeoff between weight efficiency and target performance. Figure 6 shows that the baseline, NERA, and SERA targets impacted with obliquity demonstrated a similar ballistic efficiency as monolithic RHA plates tested with no obliquity.

Between the two variants of semi-energetic targets, the 50/50 Al/PTFE mix resulted in slightly smaller residual masses, which indicate better armor performance. These results indicate there may be a small advantage to mixtures of Al-PTFE that are closer to a stoichiometric balance and react at faster rates.

The residual masses of the plates were also examined. Front plates were found to have lost slightly more mass during penetration than the back plates did. This is not surprising because once the projectile perforates the front plate it has less kinetic energy to perforate the back plate. The plates of the NERA targets were not analyzed because many of the bolts holding them together were completely stripped and/or the nut was friction welded to the bolt.

4.2 Deflagration Velocity

The technique for measuring the burn velocity of the energetic materials was successful. The break-wire data was used to correctly validate the location of the impact and thus the location of the reaction's origin. Prior research by the Army Research Laboratory on stoichiometric-balanced Al-PTFE (26% Al, 74% PTFE) shows that the deflagration-to-detonation transition of Al-PTFE occurs at roughly 5100 feet/sec (speed of sound in a 2.29 g/cm³ tile of Al-PTFE) [1]. The reaction velocities observed in the present testing were roughly half of that, so the reactions were certainly deflagrations rather than detonations. This was the intended reaction, but it appears to have been too slow to drive the front flyer plate and affect the incoming projectile.

Reaction velocities were observed to decrease as the reaction progressed. This is credited to two factors: loss of confinement as the reaction approached the edge of the plate, and dissipation of the impact energy through the target. Research by ARL suggested that Al-PTFE "requires a mechanical stimulus not only to initiate the reaction, but also to sustain it." [1]

4.3 High Speed Video

High speed video is often helpful for developing an understanding of complex dynamic events. Within 200 microseconds after impact, the SERA targets clearly show an energetic reaction, where the NERA and baseline targets do not. Based on the high-speed video, it appears that the 50/50 Al-PTFE mix reacts faster than the 70/30 Al-PTFE mix, which was expected. Burn velocity measurements, however, indicate that their burn rates were rather similar. The reaction of the 50/50 Al-PTFE mix appears to begin as the projectile is still within the armor (+105 μ s, Figure 8) where the reaction of the 70/30 Al-PTFE mix only becomes evident once the projectile has fully perforated the armor (+271 μ s, Figure 9). In both cases, the reaction appears to have happened too slowly to drive the front flyer plate into the path of the projectile. Front plate motion doesn't occur until the tail of the projectile has passed through the target.

4.4 Real Time Video

The real-time video was captured in high-definition and is stored in Ben Langhorst's testing files. It shows that impacts with the SERA targets are brighter and more exciting looking, but not significantly more violent than the NERA and baseline targets. All targets were much less violent than explosive-reactive armor targets would have been.

5. CONCLUSIONS

The SERA concept behaved as expected—burning violently rather than detonating and burning completely rather than throwing pieces of unreacted material around the test arena. Burn velocities were calculated for the specific energetic materials that were used and the evolution of the reactions was clearly recorded in high speed photography. However, the reaction appears to have happened too slowly to affect the incoming projectile. Front plate motion occurred largely after the projectile had already perforated the target. Collateral damage and reaction violence were much lower than can be expected from explosive reactive armor systems.

The NERA concept reacted less violently than expected upon impact. Some bolts broke, but targets remained largely intact and the perimeter of the rubber remained compressed. Further, front and rear plate petaling was only marginally more pronounced than the petaling observed in the uncompressed rubber targets.

As a result, the SERA and NERA systems did not significantly outperform baseline uncompressed rubber armor systems. When compared to monolithic RHA tested with no obliquity, the systems all seem to exhibit similar ballistic efficiency.

Nonetheless, the functionality of the SERA system was very positive and the concept may be worthy of additional development. It is expected that the efficiency of the SERA armor systems could be improved by engineering any combination of three changes to the system design:

1. Confining the energetic reaction in compartments that force expansion to occur in the target-thickness direction (pushing the front and rear plates apart) and significantly reducing the volume of reaction products that can escape out the sides of the target.
2. Pre-igniting the energetic material so that its reaction begins early and the front plate can begin to move before the projectile arrives at the front plate.
3. Increasing the burn velocity of the energetic material so that it can throw the front plate fast enough to interact with the rear of the projectile before the projectile entirely passes through the target.

6. REFERENCES

- [1] D.T.Casem, "Mechanical Response of an AL-PTFE Composite to Uniaxial Compression Over a Range of Strain Rates and Temperatures", Army Research Laboratory, Aberdeen Proving Ground, MD, 2008
- [2] M.Held, "Schutzeinrichtung gegen Geschosse, insbesondere Hohlladungsgeschosse (Protection Device Against Projectiles, Especially Shaped Charges)", Deutsches Patent 2 358 277, (1973)
- [3] M.Held, "Disturbance of Shaped Charge Jets by Bulging Armor", Propellants, Explosives, Pyrotechnics, 2001, Vol. 26, pp. 191-195
- [4] B.Langhorst, T.M.Lillo, H.S.Chu, "A Residual Mass Ballistic Testing Method to Compare Armor Materials or Components", Journal of Testing and Evaluation, in press

APPENDIX A

Ballistic Log Sheet													
Date	Wednesday, July 17, 2013			Time					Temperature	90oF			
Project	SERA/NERA Testing				Gun	30mm			Wind	5-10mph from South			
Personnel	Pls Ben			121 Inches from muzzle to center of light screens 125 Inches from center of light screens to target 193 Inches from camera lens to target 236 Inches from camera lens to fiducial board Camera used for velocities (lens) Camera used for wide view (lens) Chronograph used									
	Gun operators Timmy and James												
	Others Nikki, Andrew, Tom Zegula												
Velocity Measurements	3xM57 + M83 CHRONOGRAPH												
Other instrumentation	meDAQ with 6 channels												
Time	Shot no.	Projectile Name	Grains	Primer Name	Grains	Powder Name	Grains	Barrel temp (oF)	Velocity (feet/sec)	(m/sec)	Target	RRM	Comments
10:39:29 AM	1	5-inch rod	1946	Factory	59	IMR-4895	2500		3566		0.75" RHA dummy target at 60deg		hit top edge of target, rod not found
10:53:00 AM	2	5-inch rod	1946	Factory	59	IMR-4895	2500		3605		uncompressed rubber A	904	
11:22:34 AM	3	5-inch rod	1946	Factory	59	IMR-4895	2500		3634		uncompressed rubber B		no rod found
11:33:29 AM	4	5-inch rod	1946	Factory	59	IMR-4895	2500		3595		uncompressed rubber C	764	hit plate***
11:45:39 AM	5	5-inch rod	1946	Factory	59	IMR-4895	2500		3579		compressed rubber A	808	
11:59:23 AM	6	5-inch rod	1946	Factory	59	IMR-4895	2500		3631		compressed rubber B	834	
12:10:09 PM	7	5-inch rod	1946	Factory	59	IMR-4895	2500		3587		compressed rubber C	870	
12:29:26 PM	8	5-inch rod	1946	Factory	59	IMR-4895	2500		3592		70/30 A/PTFE A	804	
2:17:16 PM	9	5-inch rod	1946	Factory	59	IMR-4895	2500		3666		70/30 A/PTFE B	894	4 break-lines, 2" apart, 1-4 are at rows 2.5, 3.5, 4.5, 5.5 (bottom row is 1)
2:37:35 PM	10	5-inch rod	1946	Factory	59	IMR-4895	2500		3605		70/30 A/PTFE C	766	6 break-lines, 2" apart, 1-6 are at rows 6.5, 5.5, 4.5, 3.5, 2.5, 1.5 (bottom row is 1)
2:57:38 PM	11	5-inch rod	1946	Factory	59	IMR-4895	2500		3613		50/50 A/PTFE A	1314	
3:17:07 PM	12	5-inch rod	1946	Factory	59	IMR-4895	2500		3623		50/50 A/PTFE B	762	6 break-lines 2" apart, 1-6 are at rows 6.5, 5.5, 4.5, 3.5, 2.5, 1.5 (bottom row is 1)
3:37:41 PM	13	5-inch rod	1946	Factory	59	IMR-4895	2500		3642		50/50 A/PTFE C	850	

Shot #9 – Burn Velocity Data

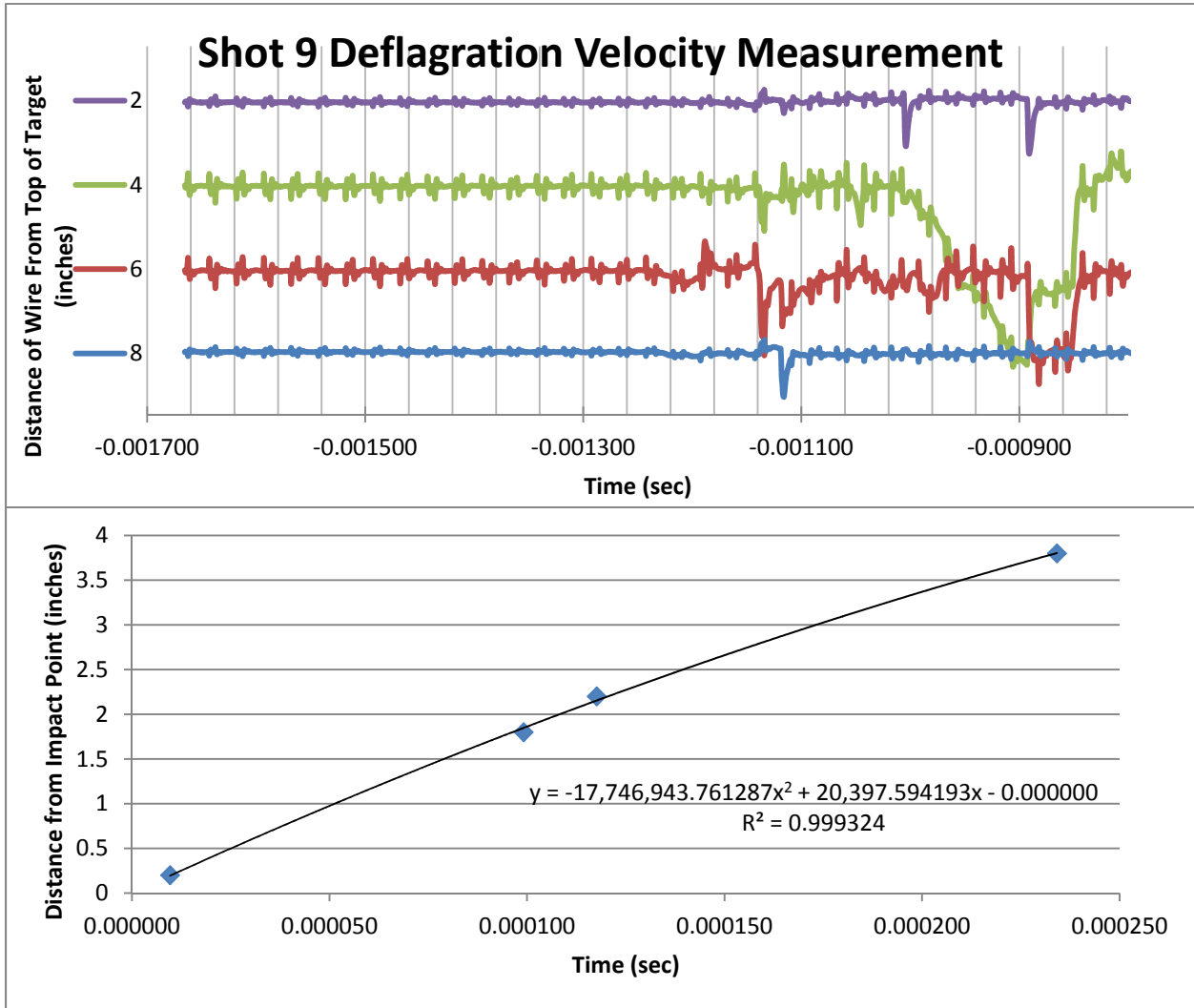


Figure 10. Front and back plates from a shot 70/30 SERA target with lines depicting where break lines were positioned.

Shot #10 – Burn Velocity Data

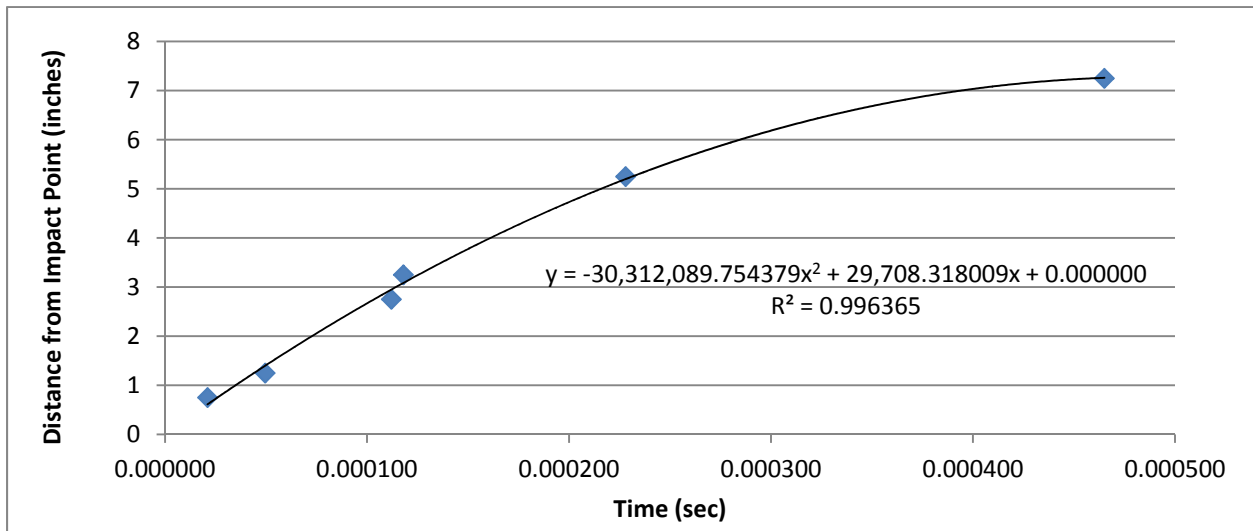
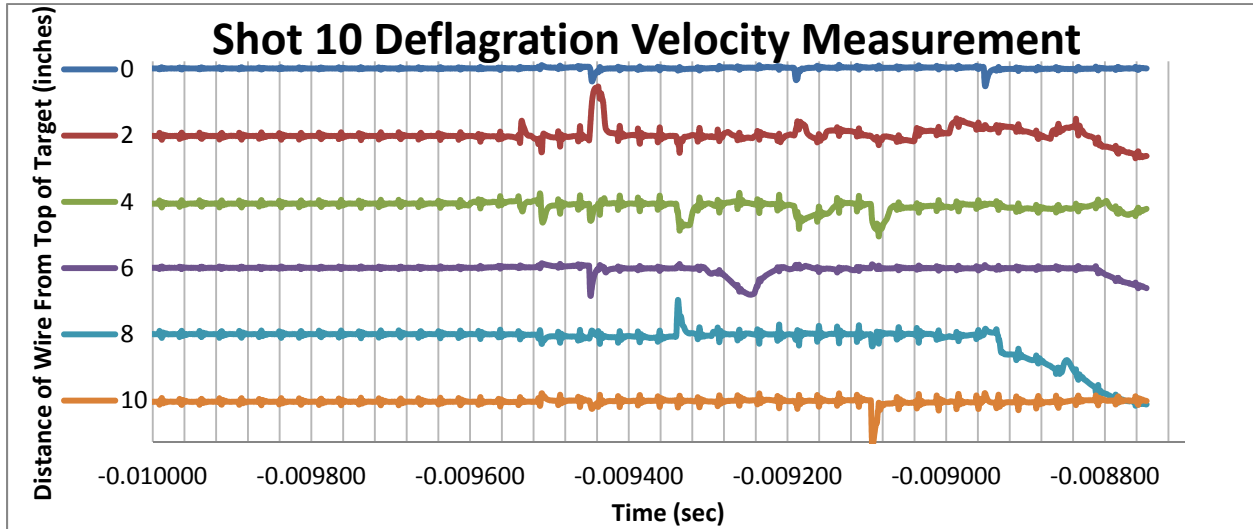


Figure 11. Front and back plates from a shot 70/30 SERA target with lines depicting where break lines were positioned

Shot #12 – Burn Velocity Data

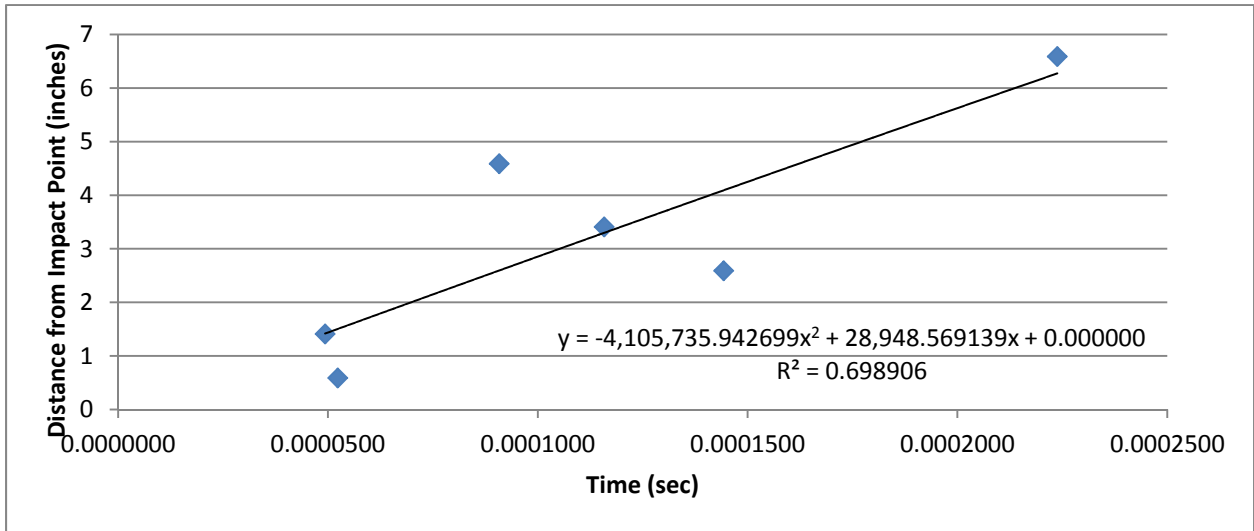
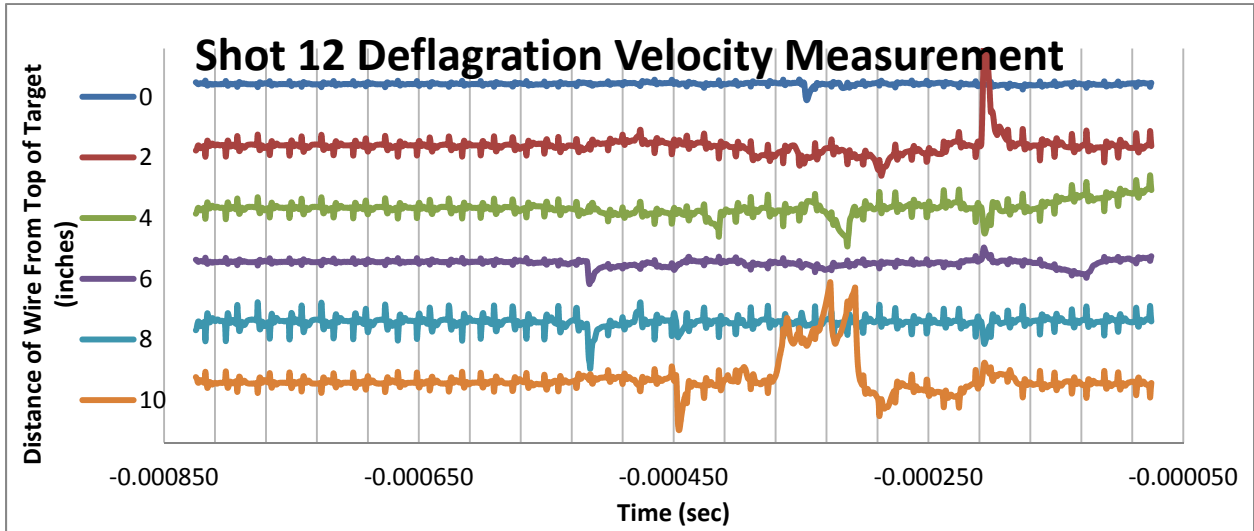


Figure 12. Front and back plates from a shot 50/50 SERA target with lines depicting where break lines were positioned.